

On the Performance of Handover Mechanisms for Non-Terrestrial Networks

Yusuf Islam Demir^{*†}, Muhammad Sohaib J. Solaija^{*}, and Hüseyin Arslan^{*‡}

^{*}Department of Electrical and Electronics Engineering, Istanbul Medipol University, Istanbul, 34810 Turkey

[†]Department of Electrical and Electronics Engineering, Istanbul University-Cerrahpaşa, Istanbul, 34320 Turkey

[‡]Department of Electrical Engineering, University of South Florida, Tampa, FL 33620 USA

Email: yusuf.demir@medipol.edu.tr, solaija@ieee.org, huseyinarslan@medipol.edu.tr

Abstract—Next-generation wireless networks require massive connectivity and ubiquitous coverage, for which non-terrestrial networks (NTNs) are a promising enabler. However, NTNs, especially non-geostationary satellites bring about challenges such as increased handovers (HOs) due to the moving coverage area of the satellite on the ground. Accordingly, in this work, we compare the conventional measurement-based HO triggering mechanism with other alternatives such as distance, elevation angle, and timer-based methods in terms of the numbers of HOs, ping-pong HOs, and radio link failures. The system-level simulations, carried out in accordance with the 3GPP model, show that the measurement-based approach can outperform the other alternatives provided that appropriate values of hysteresis/offset margins and time-to-trigger parameters are used. Moreover, future directions regarding this work are also provided at the end.

Index Terms—5G, 6G, handover (HO), low-Earth orbit (LEO), non-terrestrial network (NTN), radio link failure (RLF), satellite.

I. INTRODUCTION

Fifth generation (5G) wireless networks have shifted the focus from high data rates to increased coverage, massive connectivity, high reliability, low latency, high mobility, and better power efficiency. All these requirements are expected to be escalated even further with the introduction of sixth generation (6G) networks [1], [2]. As such, the deployment of non-terrestrial networks (NTNs) is becoming an increasingly popular approach to address the connectivity outage as the users look for reliable and ubiquitous service irrespective of the location [3]. However, despite its advantages related to speedy and flexible deployment NTN brings about its own unique challenges such as propagation channel and delay, frequency/bandwidth plan, link budgeting, mobility of the satellite, and user equipments (UEs) [4].

Mobility is challenging even for conventional terrestrial networks because it leads to issues such as Doppler spreading, time selectivity of the channel, and increased handovers (HOs) [5]. These problems are further compounded in low Earth orbit

This work was supported by the Scientific and Technological Research Council of Turkey (TÜBİTAK) under Grant 5200107, with the cooperation of Turkcell Technology and Istanbul Medipol University.

This work has been submitted to the IEEE for possible publication. Copyright may be transferred without notice, after which this version may no longer be accessible.

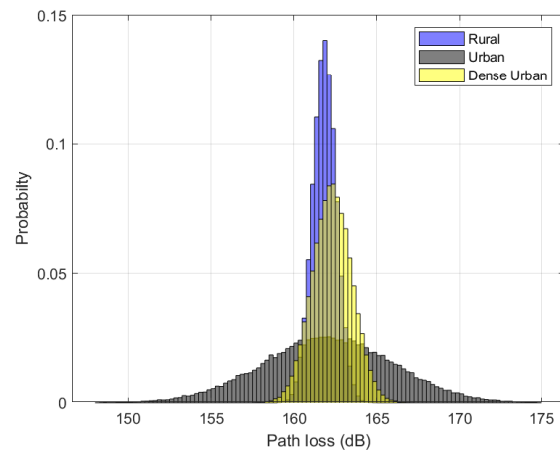


Fig. 1. Comparison of the path loss for different environments for cell diameter of 50km and NTN altitude of 600km.

(LEO) satellites since their footprint can vary with speeds up to 7.56 km/s [6] which is significantly faster than terrestrial user mobility (for comparison, high-speed trains move with speeds around 0.14 km/s). Even with the larger footprints of NTNs, their speed potentially causes an increased number of HOs. Moreover, the propagation distance from the satellite to ground can be much higher compared to coverage footprint, which would lead to reduced received signal strength (RSS) variation in these networks compared to terrestrial networks [6]. This predicament is illustrated for different environments in Fig. 1. While urban environment still exhibits an RSS range of around 20 dB, this variation is limited to 4 – 5 dB in rural and dense urban environments.

In conventional (terrestrial) networks, the users are handed over from one cell or eNodeB to another based on measured RSS, reference signal received power (RSRP), or reference signal received quality (RSRQ). Specifically, in the case of A3 events, the HO is triggered when the received signal of the neighboring eNodeB (eNB) is a certain threshold (hysteresis) stronger than the serving one for a specific amount of time [7]. However, with the reduced RSS variation in NTNs the efficacy of the measurement-based HO mechanisms could be compromised.

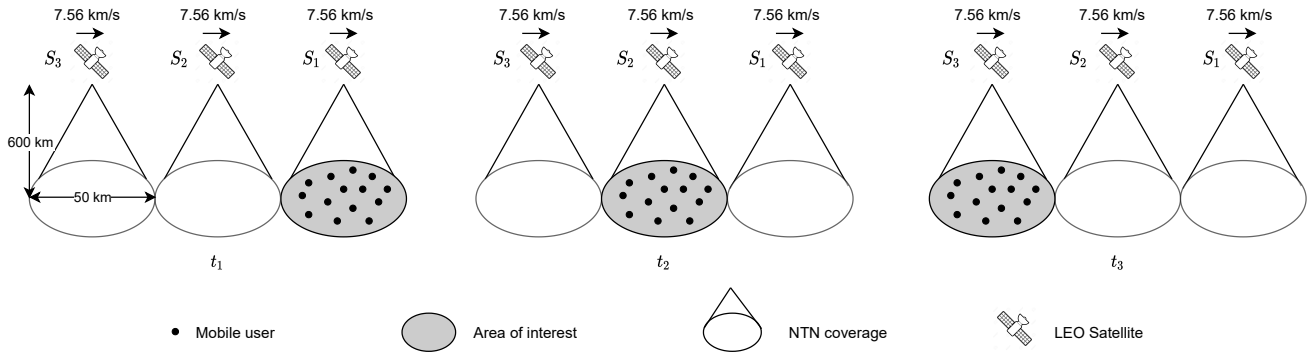


Fig. 2. Illustration of the considered scenario.

Accordingly, some recent works have looked at different aspects of this problem. The general trends related to LEO satellites HO mechanisms are provided in [8], with the authors highlighting the need for content and device-specific approaches in future networks. The performance of conventional HO mechanism in LEO-based NTN is compared against two terrestrial scenarios, i.e., urban macro and high-speed train in [9], with the results showing that the performance is significantly degraded in terms of outage, HOs and radio link failures (RLFs). The achievable data rates/capacity for millimeter wave (mmWave) band operation in NTN is studied in [10]. In [11], authors suggest and analyze the use of fixed-beam LEO satellites to mitigate the excessive HOs in the case of moving beams. Recent releases of 3rd Generation Partnership Project (3GPP) specifications have also considered conditional handover (CHO) as potential improvement of the conventional HO methods, and [12] studies the effect of different values of parameters such as add, remove, replace, and execution offset and its impact on HOs and RLFs.

However, none of the works mentioned above have evaluated any alternatives to the conventional HO mechanisms so far. Accordingly, in this work, we first provide an implementation of the alternative handover mechanisms suggested in [6]. Moreover, we carry out a simulation-based comparative analysis of these mechanisms, i.e., distance/position, elevation angle, and timer-based methods. The performance of these methods is evaluated in terms of the number of HOs, ping-pong handovers (PP HOs), and RLFs and benchmarked against the conventional measurement-based approach.

The rest of this paper is organized as follows. Section II describes the system model used in this study, the alternative HO mechanisms are discussed in Section III, simulation results are provided in Section IV while conclusions and future directions are provided in Section V.

II. SYSTEM MODEL AND ASSUMPTIONS

In this work we assume a single circular cell on the ground with outdoor users randomly distributed inside the cell, while three LEO satellites move overhead, as shown in Fig. 2. The simulation is assumed to start at time t_1 where satellite S_1 is right above the cell center. The LEO high-speed motion

is assumed to continue linearly at a speed of 7.56 km/s till satellite S_3 is on top of the cell center. Since our primary goal is to evaluate the performance of the different HO mechanisms in the challenging circumstances provided by NTN, we have chosen the worst case, i.e., the lowest altitude and smallest cell diameter, which are 600 and 50 km. The low altitude leads to a fast-moving coverage footprint while the small cell size leads to reduced RSS variation. In the remainder of this section, we will first describe the path loss model and its associated parameters before providing the details of the user mobility pattern used in our analysis.

A. Path Loss Model

The path loss model for NTN was developed by 3GPP in Rel-15 [4], and is reproduced below

$$PL = PL_b + PL_s + PL_g + PL_e, \quad (1)$$

where basic path loss, ionospheric/tropospheric scintillation, attenuation due to atmospheric gasses, and building entry losses (all in dB) are represented by PL_b , PL_s , PL_g and PL_e , respectively. The basic path loss is given by

$$PL_b = SF + CL + FSPL, \quad (2)$$

where $SF \sim \mathcal{N}(0, \sigma_{SF}^2)$ represents the shadow fading, CL represents the clutter loss and $FSPL$ represents the free-space path loss. The values of σ_{SF} and CL are given in Table I. The free-space path loss is given by

$$FSPL = 32.45 + 20 \log_{10}(f_c) + 20 \log_{10}(d), \quad (3)$$

where f_c represents the carrier frequency in GHz and d is the 3-D distance (in meters) between the UE and satellite calculated by

$$d = \sqrt{R_E^2 \sin^2 \alpha + h_0^2 + 2h_0 R_E - R_E \sin \alpha}, \quad (4)$$

where R_E is the radius of the Earth, α is the elevation angle and h_0 is the altitude of the satellite.

For $f_c < 6$ GHz, tropospheric scintillation is considered to be negligible while ionospheric scintillation is equivalent to $P_{fluc}/\sqrt{2}$ where P_{fluc} is a function of the S_4 scintillation parameter [13]. The absorption due to atmospheric gases, PL_g , is assumed to be negligible for $f_c < 6$ GHz, while

TABLE I
PATH LOSS PARAMETERS FOR NTNS IN DENSE URBAN SCENARIO [4]

Elevation Angle (α)	LoS Probability	Shadow Fading (σ_{SF})		Clutter Loss (CL)
		LoS	NLoS	
10°	28.2%	3.5	15.5	34.3
20°	33.1%	3.4	13.9	30.9
30°	39.8%	2.9	12.4	29.0
40°	46.8%	3.0	11.7	27.7
50°	53.7%	3.1	10.6	26.8
60°	61.2%	2.7	10.5	26.2
70°	73.8%	2.5	10.1	25.8
80°	82.0%	2.3	9.2	25.5
90°	98.1%	1.2	9.2	25.5

the building penetration loss, PL_e , is also ignored since all the users are assumed to be outdoors [4].

The overall path loss then becomes a weighted sum of the line-of-sight (LoS) and non-line-of-sight (NLoS) components and is given by [14]

$$PL_{tot} = Pr_{LoS}(\alpha) * PL_{LoS} + (1 - Pr_{LoS}(\alpha)) * PL_{NLoS}, \quad (5)$$

where $Pr_{LoS}(\alpha)$ gives the LoS probability for elevation angle α , $1 - Pr_{LoS}(\alpha)$ is the NLoS probability, and PL_{LoS} and PL_{NLoS} represent the path losses for the LoS and NLoS components, respectively.

B. User Mobility Model

In this work, both static and mobile users are considered. For mobile users, memory-based smooth random mobility model is used. As the name implies, in memory-based models a user's current state (in terms of speed and/or direction) is a function of its past state(s) which is more realistic compared to memory-less models such as random walk [15]. The model provided in [16] considers user speeds in the interval $[0, v_{max}]$, where certain speeds have higher probability while uniform distribution is used in the remaining interval. The change in direction is done after a time interval which is itself exponentially distributed. For a more detailed explanation of the model, the readers are referred to [16]. However, it should be noted that to provide a fair comparison with the static user case the user mobility had to be limited to the considered cell region. This was ensured by modifying the aforementioned model to change the user direction by a shift of π radians if it reached the cell edge.

III. ALTERNATIVE HANDOVER REALIZATIONS

In this section we describe the HO triggering mechanisms, starting from the conventional RSS-based methods before looking at other measurements such as distance, timer, and elevation angle which have been identified as potential HO triggers in 3GPP discussions [6].

A. Measurement-Based Handover

In general, measurement-based HO techniques rely on the signal strength of the received signal to trigger HOs. The specific measured quantity might change, for instance RSRP, RSRQ or received signal strength indicator (RSSI) might be

used [17]. While there are different variants of measurement-based HO triggering events, we will limit ourselves to the A3 event, which is arguably the most popular. In addition to the measured signal strength, there are some additional parameters that are used in A3 measurements, i.e., hysteresis/offset margins and time-to-trigger (TTT). Hysteresis and offset margins are used to bias the user cell association towards the serving cell by making it look stronger than its actual signal strength to avoid unnecessary HOs. In addition to this, TTT parameter dictates how long the signal strength condition lasts to avoid PP HOs. Mathematically, the measurement-based HO trigger can be written as

$$Q_t > Q_s + Q_{hys} + Q_{off}, \quad (6)$$

where Q can refer to any signal strength measurement such as RSRP, RSRQ or RSSI. However, in this work we will focus on RSS. The subscripts t and s refer to target and source cells, respectively, and Q_{hys} and Q_{off} are the respective hysteresis and offset margins. As mentioned earlier, the condition in (6) should be satisfied for a minimum of TTT duration for the HO to be triggered. The RSS is calculated as follows:

$$Q = EIRP - PL_{tot}, \quad (7)$$

where equivalent isotropically radiated power (EIRP) is a function of the transmit power and transmit antenna gain while PL is the total path loss as described in Section II-A

B. Distance/Location-Based Handover

In the distance-based approach, the initial association of the UEs is done based on the distance, i.e., the UE associates itself with the nearest satellite. This is done with the assumption that the location of the UE and NTN satellite is exactly known and the distance can be calculated from that. Similar to the measurement-based approach, we use a hysteresis margin in the distance-based method while triggering the HO condition. This can be illustrated as

$$d_t < d_s - d_{off}, \quad (8)$$

where d_t and d_s are the UE's distances from the target and source satellites, respectively, and d_{off} is the offset parameter.

C. Elevation Angle-Based Handover

Similar to the distance-based method, in elevation angle-based approach the UE is associated with the satellite that has the largest elevation angle, α . Here again we assume the availability of UE and satellite's locations which can then be used to calculate α . The former's location can be obtained using Global Positioning System (GPS) coordinates [6] while ephemeris data can be used for the latter [18]. For HO triggering, an offset parameter is used as follows:

$$\alpha_t > \alpha_s + \alpha_{off}, \quad (9)$$

where α_t and α_s are the UE's elevation angles with respect to the target and source satellites, respectively, and α_{off} is the offset parameter.

TABLE II
SIMULATION ASSUMPTIONS AND PARAMETERS

Parameter	Values
Environment	Dense Urban
NTN altitude (h_0)	600 km
Cell diameter	50 km
EIRP density	34 dBW/MHz
Carrier frequency (f_c)	2 GHz (S-Band)
Scintillation (S_4)	0.5
P_{fluc} (dB)	11
Radio link failure (RLF) parameters	$Q_{in} = -6$ dB, $Q_{out} = -8$ dB T310 timer = 500 ms
TTT (ms)	20, 40, 60, 80, 100
$Q_{hyst} + Q_{off}$ (dB)	1, 2, 3, 4
α_{off} ($^\circ$)	1, 2, ..., 10
t_{off} (s)	6.4, 6.45, ..., 6.8
d_{off} (km)	1, 1.5, ..., 5
v_{max} (m/s)	10

D. Timer-Based Handover

The timer-based HO trigger is aimed at utilizing the knowledge of the satellite speed/trajectory to predict the time duration for which the satellite's footprint covers a certain cell on the ground. For instance, considering the satellite speed as 7.56 km/s, a cell of 50 km in diameter would be covered by a particular satellite for only $50/7.56 = 6.61$ seconds. As such, it is possible to initiate a timer once the user makes its initial association with a satellite and initiate the HO after every $t_{off} \approx 6.61$ s.

As described in Section II, we assume the satellite S_1 to be in line with the cell center at time t_1 . As such, we cannot initiate the timer, t_{off} with respect to first user cell association. To maintain fairness, we use the same methodology as distance-based HO in the initial phase, i.e., before the HO from S_1 to S_2 . Once the UE is handed over to S_2 , timer t_{off} is initiated and HO to S_3 is initiated once the timer reaches its threshold.

IV. SIMULATION RESULTS AND DISCUSSION

For this work, we have considered downlink communication in S-band between LEO NTN and ground users in a dense urban scenario. In line with set-1 of the system-level simulation parameters provided in [6], we assume LEOs at an altitude, h_0 , of 600 km and EIRP density of 34 dBW/MHz. Users are randomly located with a density of ~ 1 UE/km² in the cell, where each user is allocated a single physical resource block (PRB) throughout the simulation. The cell size is chosen to be equal to the satellite beam diameter, i.e., 50 km. The noise in the system is assumed to be -121.4 dBm [19]. Table II provides a summary of these parameters as well as the offset values used in the simulations. Here it should be noted that while the hysteresis/offset values for measurement-based approaches are taken from the literature (and live network), the values for the alternative HO methods are devised heuristically after observing the ranges of these variables in the simulations.

The performance of the conventional and alternative HO triggering methods are compared in terms of the number of HOs, PP HOs, and RLFs. A PP HO is considered to have

occurred if a UE is handed over to the target cell but returns to the original serving cell within 5 seconds [17]. An RLF, on the other hand, occurs if the signal-to-interference-plus-noise ratio (SINR) of the UE falls below a certain threshold, Q_{out} , and does not exceed another threshold, Q_{in} , (where $Q_{in} > Q_{out}$) within the time duration defined by timer T310 [19]. For SINR calculation, only the interference from the other two satellites (apart from the one the user is connected to) is considered.

The performance of measurement-based HOs is summarized in Table III for different values of hysteresis/offset margins and TTT parameter. As expected, the number of HOs decreases, and RLFs increase with the increase in hysteresis/offset margins and TTT values. However, it is interesting to note that for both, static and mobile UEs the performance of the system is nearly identical. This is because the mobility of LEO satellite itself is much higher than the user mobility (7.56 km/s vs 10 m/s). Additionally, there are certain values of the HO parameters (TTT = 20, $Q_{hyst} + Q_{hyst} = 3$; TTT = 40, $Q_{hyst} + Q_{hyst} = 2$; TTT = 60, $Q_{hyst} + Q_{hyst} = 1$) where the number of both ping-pong HOs and RLFs are zero. Table IV evaluates the alternative HO mechanisms described in Section III. Similar to the measurement-based approach, the number of HOs decreases, and RLFs increase with the increase in offset values for distance and elevation angle-based methods. In fact, for $\alpha_{off} = 10^\circ$ the number of HOs becomes zero. However, as mentioned earlier, this comes at the cost of increased RLFs. Additionally, it is interesting to note that even at low offset values, there is no ping-pong effect. This is due to the fact that unlike RSS, where there is some randomness in the form of shadow fading, there is negligible randomness (due to the disparity in mobility levels of UEs and satellites) effect for distance, angle or timer-based approaches. Moreover, it is observed that for zero ping-pong and RLF cases, the number of HOs in the alternative approaches is significantly higher compared to the measurement-based approach. This indicates that the conventional HO triggering scheme still performs well in an NTN scenario and can be used in the next generation NTNs.

V. CONCLUSION AND FUTURE DIRECTIONS

The increasing need for ubiquitous connectivity, coupled with cost-effective satellite solutions driven by private ventures has led to a flurry of activity around NTNs from an industrial as well as standardization perspective. However, NTNs and particularly LEO satellites introduce additional challenges including mobility of the satellite itself, leading to increased HOs. Furthermore, the reduced RSS variation in these networks compared to their terrestrial counterparts calls for investigation of new HO mechanisms. In this paper, we have compared the performance of conventional measurement-based HOs with alternatives such as location/distance, elevation angle, and timer-based methods in terms of numbers of HOs, PP HOs and RLFs. Our analysis indicates that the conventional HO mechanism can still outperform these alternatives provided that proper selection of parameters is

TABLE III

PERFORMANCE COMPARISON OF MEASUREMENT-BASED HANDOVER SCHEME FOR DIFFERENT HYSTERESIS/OFFSET MARGINS AND TTT VALUES

TTT (ms)	$Q_{hyst} + Q_{off}$ (dB)	Static User			Mobile User		
		HOs	PP HOs	RLFs	HOs	PP HOs	RLFs
20	1	28426	13318	0	28550	13386	0
	2	9966	16	0	9994	26	0
	3	9606	0	0	9615	0	0
	4	9291	0	5	9307	0	6
40	1	9719	8	0	9738	3	0
	2	9411	0	0	9450	0	0
	3	8944	0	50	8941	0	62
	4	7784	0	1211	7749	0	1253
60	1	9421	0	0	9422	0	0
	2	9009	0	29	8985	0	30
	3	7931	0	1009	7915	0	1025
	4	1668	0	4105	1674	0	4092
80	1	9188	0	1	9194	0	2
	2	8482	0	307	8521	0	317
	3	3869	0	3230	3966	0	3228
	4	131	0	4615	137	0	4630
100	1	8953	0	29	8919	0	22
	2	7517	0	1241	7611	0	1264
	3	1004	0	4332	997	0	4336
	4	9	0	4675	16	0	4671

TABLE IV

PERFORMANCE COMPARISON OF DIFFERENT HANDOVER MECHANISMS

	Offset	Static User			Mobile User		
		HOs	PP HOs	RLFs	HOs	PP HOs	RLFs
Distance-Based (km)	1	14655	0	0	14656	0	0
	1.5	13524	0	0	13523	0	0
	2	11149	0	0	11149	0	0
	2.5	9572	0	255	9572	0	271
	3	8594	0	970	8594	0	1012
	3.5	7990	0	1627	7991	0	1684
	4	7830	0	2194	7830	0	2254
	4.5	7648	0	2547	7648	0	2598
	5	7385	0	2893	7385	0	2969
	Elevation Angle-Based (α)	1°	15460	0	0	15459	0
2°		14990	0	0	14990	0	0
3°		14273	0	0	14274	0	0
4°		13232	0	0	13231	0	0
5°		7831	0	2191	7831	0	2250
6°		7501	0	2739	7501	0	2808
7°		6971	0	3316	6971	0	3351
8°		6175	0	3857	6175	0	3837
9°		4952	0	4297	4952	0	4308
10°		0	0	4679	0	0	4678
Timer-Based (s)	6.4	15708	0	0	15708	0	0
	6.45	15708	0	0	15708	0	0
	6.5	15708	0	0	15708	0	0
	6.55	15708	0	0	15708	0	0
	6.6	15708	0	0	15708	0	0
	6.65	15706	0	0	15706	0	0
	6.7	15699	0	0	15699	0	0
	6.75	15690	0	0	15690	0	0
6.8	15681	0	0	15681	0	0	

made. However, here we would like to reiterate that for the purpose of this work we have only considered a homogeneous NTN, i.e, the terrestrial network or satellites at different altitudes/orbits have not been considered. Additionally, we have not looked at the feasibility or the possible errors in obtaining the measurements such as elevation angle, location or distance. Rather, these aspects are left as a future study.

ACKNOWLEDGMENT

The authors would like to acknowledge and express their gratitude for valuable suggestions provided by A. E. Duranay and M. İ. Sağlam during the preparation of this manuscript.

REFERENCES

- [1] Z. Zhang, Y. Xiao, Z. Ma, M. Xiao, Z. Ding, X. Lei, G. K. Karagiannis, and P. Fan, "6G wireless networks: Vision, requirements, architecture, and key technologies," *IEEE Vehicular Technology Magazine*, vol. 14, no. 3, pp. 28–41, 2019.
- [2] S. Dang, O. Amin, B. Shihada, and M.-S. Alouini, "What should 6G be?" *Nature Electronics*, vol. 3, no. 1, pp. 20–29, 2020.
- [3] M. Giordani and M. Zorzi, "Non-terrestrial networks in the 6G era: Challenges and opportunities," *IEEE Network*, 2020.
- [4] 3rd Generation Partnership Project (3GPP), "Study on New Radio (NR) to support non-terrestrial networks (Release 15)," Technical Report 38.811, ver 15.4.0, Sept. 2020.
- [5] J. Wu and P. Fan, "A survey on high mobility wireless communications: Challenges, opportunities and solutions," *IEEE Access*, vol. 4, pp. 450–476, 2016.
- [6] 3rd Generation Partnership Project (3GPP), "Solutions for NR to support non-terrestrial networks (NTN) (Release 16)," Technical Report 38.821, ver 16.1.0, May 2021.
- [7] —, "Radio Resource Control (RRC) protocol specification (Release 16)," Technical Specification 38.831, ver 16.7.0, Dec. 2021.
- [8] S. Park and J. Kim, "Trends in LEO Satellite Handover Algorithms," in *IEEE 12th International Conference on Ubiquitous and Future Networks (ICUFN)*, 2021, pp. 422–425.
- [9] E. Juan, M. Lauridsen, J. Wigard, and P. E. Mogensen, "5G New Radio Mobility Performance in LEO-based Non-Terrestrial Networks," in *IEEE Globecom Workshops (GC Wkshps)*, 2020, pp. 1–6.
- [10] M. Giordani and M. Zorzi, "Satellite communication at millimeter waves: A key enabler of the 6G era," in *IEEE International Conference on Computing, Networking and Communications (ICNC)*, 2020, pp. 383–388.
- [11] J. S. Baik and J.-H. Kim, "Analysis of the Earth Fixed Beam Duration in the LEO," in *IEEE International Conference on Information Networking (ICOIN)*, 2021, pp. 477–479.
- [12] H. Martikainen, I. Viering, A. Lobinger, and T. Jokela, "On the basics of conditional handover for 5G mobility," in *IEEE 29th Annual International Symposium on Personal, Indoor and Mobile Radio Communications (PIMRC)*, 2018, pp. 1–7.
- [13] International Telecommunication Union (ITU), "Ionospheric propagation data and prediction methods required for the design of satellite networks and systems," Recommendation ITU-R P.531-14, Aug. 2019.
- [14] A. Al-Hourani, S. Kandeepan, and S. Lardner, "Optimal LAP altitude for maximum coverage," *IEEE Wireless Communications Letters*, vol. 3, no. 6, pp. 569–572, 2014.
- [15] H. Tabassum, M. Salehi, and E. Hossain, "Fundamentals of Mobility-Aware Performance Characterization of Cellular Networks: A Tutorial," *IEEE Communications Surveys Tutorials*, vol. 21, no. 3, pp. 2288–2308, 2019.
- [16] R. R. Roy, "Smooth random mobility," in *Handbook of Mobile Ad Hoc Networks for Mobility Models*, R. R. Roy, Ed. Boston, MA, USA: Springer, 2011, ch. 5, pp. 125–165.
- [17] R. Ahmad, E. A. Sundararajan, N. E. Othman, and M. Ismail, "Handover in LTE-advanced wireless networks: state of art and survey of decision algorithm," *Telecommunication Systems*, vol. 66, no. 3, pp. 533–558, 2017.
- [18] O. Liberg, S. E. Löwenmark, S. Euler, B. Hofström, T. Khan, X. Lin, and J. Sedin, "Narrowband Internet of Things for Non-Terrestrial Networks," *IEEE Communications Standards Magazine*, vol. 4, no. 4, pp. 49–55, 2020.
- [19] O. N. Yilmaz, J. Hämäläinen, and S. Hämäläinen, "Optimization of adaptive antenna system parameters in self-organizing LTE networks," *Wireless Networks*, vol. 19, no. 6, pp. 1251–1267, 2013.